J Mater Sci: Mater Med (2014) 25:2069–2081
DOI 10.1007/s10856-014-5251-z

Protective Ag:TiO_2 thin films for pressure sensors in orthopedic prosthesis: the importance of composition, structural and morphological features on the biological response of the coatings

C. Lopes · P. Fonseca · T. Matamá · A. Gomes · C. Louro · S. Paiva · F. Vaz

Received: 17 March 2014 / Accepted: 3 June 2014 / Published online: 17 June 2014

Abstract DC reactive magnetron sputtered Ag:TiO_2 nanocomposite thin films were developed to be used as protective coatings in pressure sensor devices. The coatings, with Ag content varying from 0 to about 30 at.%, were prepared and characterized in order to study their biological response. The as-deposited samples were annealed in vacuum at 500 °C in order to evaluate the influence of their morphological and structural differences over the response elicited upon contact with simulated bodily fluids and cultured human cells, as well as selected microorganisms. The results showed that the annealing treatment produced less porous films with an enhanced structure, with a significant reduction in structural defects and improved crystallinity. Additionally, samples with higher Ag contents (≥12.8 at.%) exhibited Ag agglomerates/clusters at the surface, a result anticipated from the XRD data. The crystallization of the TiO_2 matrix was also observed by XRD analysis, albeit delayed by the dispersion of Ag into the matrix. Biological characterization showed that the antimicrobial activity and cytotoxicity of the coatings were directly related with their composition, closely followed by the particular structural and morphological features, namely those resulting from annealing process.

C. Lopes · P. Fonseca · F. Vaz (✉)
Centro de Física, Universidade do Minho, 4710-057 Braga, Portugal
e-mail: fvaz@fisica.uminho.pt

P. Fonseca · C. Louro
SEC-CEMUC, Universidade de Coimbra, 3030-788 Coimbra, Portugal

T. Matamá · A. Gomes · S. Paiva
CBMA, Universidade do Minho, 4710-057 Braga, Portugal

1 Introduction

The present work emerges from the need to create protective layers for biosensors devices, capable of monitoring pressure fields at the prosthesis/limb interface, in order to optimize the use of the prosthesis by the amputees. These layers should protect the strain sensors without affecting the operating principle for which were designed. This requires special properties as high corrosion and wear resistance, good mechanical behavior and also chemical and thermal stability. Furthermore, it is of utmost importance being innocuous for the patient since the surface sensor will be in direct contact with the human stump. This last requirement also presupposes others sensor surface characteristics, for instances being biocompatible, electrically insulator and capable of preventing fungus, yeasts and bacteria proliferation, favored in bodily fluids such as human sweat.

In the past years, titanium oxide films have been extensively used for biomedical applications owing to their biocompatibility, chemical and mechanical stability, non-toxicity and non-absorption [1]. Furthermore, over the last decade several authors reported on the excellent photocatalytic properties of the TiO_2 suggesting its potential in the healthcare sector for controlling infections upon UV light irradiation [2, 3]. Thus, TiO_2 could be an excellent candidate for biosensors protective layers. However, the titanium oxide is a relatively brittle material, which may restrict its use on applications where some ductility is required, as is the case of polymer sensors. Moreover, biopotential electrodes would greatly benefit if some level of bactericide effect could be presented, in spite of the good TiO_2 biocompatibility. Silver addition to TiO_2-based system could fulfil these requirements, enabling the tailoring of the films elastic modulus (reducing stiffness) and, simultaneously, a strong antibacterial activity against many

kinds of bacteria even at lower concentrations. However, the excellent Ag electrical performance [2, 4] could be a drawback by allowing the electrical conduction along the dielectric matrix. Thus, the chemical modification of the devices surface must be strictly controlled to prevent residual currents from being transmitted to the patient.

It is well known that silver nanoparticles, Ag-NPs, have unique chemical and physical characteristics leading to advanced magnetic, electrical, optical, mechanical and structural properties when compared to the original bulk materials. This work, focused on the broad-spectrum of antimicrobial properties of Ag NPs, widely used in health care, medical devices and surgical instruments [1, 5–7]. Furthermore, Foster et al. [3] showed that Ag:TiO_2 films display good biocidal activity against hospital related pathogens. Nevertheless, Ag-NPs have recently been considered a potential risk to biological organisms, including humans, and to the environment [6–12]. Although the toxicity of Ag-NPs is partly explained by the release of Ag^+ ions, it remains unclear if Ag-NPs are a direct cause of the enhanced toxicity. Several authors [6, 8] concluded that growth inhibition and cell damage could be directly attributed either to the NPs themselves or to the ability of Ag-NPs to deliver dissolved Ag^+ to critical biotic receptors. Growing evidence suggest that the antibacterial activity of Ag-NPs depends simultaneously on their size and surface area; it is also clear that the remarkably higher surface to volume ratio of NPs enhances the surface properties and thereby increases the interaction with biological fluids (e.g. serum, saliva or mucus) [6]. Previous toxicological studies did not conclusively establish the toxicity of NPs, as reflected in a report published by the *Scientific Committee on Emerging and Newly Identified Health Risks* (*SCENIHR*) that concluded, from the existing studies, that NPs might have different toxicological properties from the bulk substance, but their risks should be assessed on a case-by-case basis [6].

The aim of this research was twofold (i) the production of Ag:TiO_2 sputtered films with different compositions, structural and morphological features; (ii) the assessment of in vitro biocompatibility and the antimicrobial activity of the coatings. For that two routes were selected, after deposition and after heat treatment at 500 °C/60 min.

2 Experimental details

2.1 Preparation and microstructural characterization of coatings

Ag:TiO_2 thin films were deposited by reactive DC magnetron sputtering, onto silicon (100) and Pilkington® glass slides—in accordance with ISO 8037 norm for in vitro tests—the depositions were carried out in an mixture Ar/O_2 atmosphere, injected into a laboratory-sized deposition chamber. Constant fluxes of 60 and 9 sccm, corresponding to Ar and O_2 partial pressures of 0.3 Pa and 0.08 Pa, respectively, were used. The base pressure close to 2×10^{-4} Pa and the final working pressure ($\sim$0.38 Pa) were kept constant during the entire coatings deposition process. The films were synthetized with the substrate holder positioned at 70 mm from a pure (99.96 at.% of purity) Ti target ($200 \times 100 \times 6$ mm), combined with different numbers of Ag pellets ($\sim$60 mm^2 surface area and $\sim$2 mm thickness), symmetrically incrusted in the preferentially target eroded zone (to obtain different Ag concentrations). The coatings were grown in rotation mode (7 rpm) with a constant substrate bias voltage of −50 V. The target was powered with a current density of 100 A/m^2. The deposition temperature and time were set to approximately 150 °C and 2 h, respectively.

As-deposited coatings were annealed in a secondary vacuum furnace, after evacuation to about 10^{-4} Pa. The selected temperature was 500 °C and the isothermal period was fixed to 60 min, after a heating ramp of 5 °C/min. After annealing, the samples were cooled down freely, in vacuum, before their removal to room conditions. The thermal treatment parameters were selected according to previous studies [13, 14].

A Cameca SX-50 Electron Probe Microanalysis (EPMA) apparatus, operating at 15 keV, was used to determine the coatings chemical composition. The results presented in this work are an average of four random points of the films surface. Scanning electron microscopy (SEM) analysis, by using a FEI Quanta 400F apparatus at 15 keV, was used to determine the thickness and hence the deposition rate of the films. This technique was also used to probe the main morphological features of the cross-section coatings. The topography and the roughness characteristics were assessed using a Veeco di Innova Atomic Force Microscope (AFM). The measurements were performed with variable scan rate (0.6–0.8 Hz) over areas of 10×10 μm^2 and 5×5 μm^2 and the images obtained analyzed with a Gwiddion software, in order to determine the average and the mean square roughness of the post-deposited and post-annealing films.

The structural analysis was made by X-ray Diffraction (XRD), using a Philips X'Pert PW 3020/00 diffractometer, operating in a Bragg–Brentano configuration in grazing incidence mode with Co-Kα radiation. The structural parameters were obtained by deconvolution of the XRD patterns, assuming Voigt functions.

2.2 Biological characterization of coatings

The ability of the post-deposited and the post-annealed films to inhibit bacterial growth on liquid extracts, was assessed using a turbidimetric method. The media

conditioning was performed in two consecutive "washing cycles" of each material after they had been sterilized, first in 70 % ethanol and then in sterile water. Each cycle consisted in 5 days-incubation at 37 °C of each material (2.25 cm^2) with 2 mL of Nutrient Broth (complete medium for bacteria) or Yeast Extract Peptone Dextrose (yeast complete medium). The test microorganisms used were *Escherichia coli* K12, *Staphylococcus aureus* ATCC 6538 and *Candida albicans* ATCC 18804. All the inocula were grown overnight and were diluted in the adequate broths/extracts to an optical absorbance of 0.01 at 600 nm (bacteria) or of 640 nm (yeast). Incubations were carried out in a 96-wells plate at 200 rpm for at least 360 min, at 37 °C for both bacteria; and at 30 °C, for *C. albicans*. Two controls were performed: the death control contained kanamycin (bacteria)/fluconazole (yeast) and the negative control, NC, used extract from glass samples. The last one was selected for representing a similar surface known to allow mammalian cell growth. The microorganism growth was monitored by the optical density at 600/640 nm over time and corrected for the background absorbance of each blank (broths/extracts not inoculated), using a SpectraMax 340 PC spectrophotometer. The specific growth rate (min^{-1}) was obtained from the exponential time points for each growth curve and related to the specific growth rate (min^{-1}) of the glass control as percentage.

The cytotoxicity evaluation of the thin films was performed using two distinct methods and two different cell lines. The samples were cut into squares so that they could fit inside a well of a 24-wells plate (1 cm^2). The samples were sterilized in 70 % ethanol, washed three times in PBS and then allowed to dry at room temperature (inside a vertical laminar air flow cabinet). The indirect contact assay was performed with the primary cell culture of mouse embryonic fibroblasts (MEFs) to test the general toxicity of materials. The medium conditioning was performed by incubating each material with 600 μL of cell culture medium (Dulbecco's modified Eagle's medium supplemented with 10 % (v/v) Fetal Bovine Serum and 1 % (v/v) of penicillin/streptomycin), either 24 h or 5 days at 37 °C under 5 % CO_2 atmosphere. The day before the experiments, cells were seeded at a density of 10,000 cells/well on three 96-wells tissue culture plates. Cells were exposed to 100 μL of extracts and incubated during 24, 48 and 72 h, at 37 °C in a humidified atmosphere with 5 % of CO_2. Cell metabolic viability was quantified using the AlamarBlue® assay (AlamarBlue® Cell Viability Reagent, Invitrogen).

Cytotoxicity was also evaluated by a direct method, continuously, for 3 days. In this procedure, the immortalized human skin fibroblasts, BJ-5ta (ATCC CRL4001), were seeded directly on top of the material in 24-wells plates at a density of 80,000 cells/well and they were maintained in a humidified atmosphere at 37 °C and 5 % of CO_2 for three days. The medium (4 parts of Dulbecco's modified Eagle's medium, 1 part of medium 199 supplemented with 10 % (v/v) fetal bovine serum, 1 % (v/v) of penicillin/streptomycin solution and 10 μg/mL hygromycin B) was refreshed after 24 and 48 h; at these time points, the measurement of cell viability was performed by the addition of the nontoxic reagent AlamarBlue.

3 Results and discussion

3.1 Microstructural characterization

The fundamental characteristics of the four as-deposited coatings from the Ag:TiO_2 system are presented in Table 1, as well as those related to the Ti–O reference sample. Throughout the entire text the coatings will be denoted as ascribed in Table 1. A TT suffix (thermal treated) will also be introduced.

Regarding the chemical composition, EPMA analysis revealed that all coatings were chemically homogeneous with no significant variation of the constituents. The Ag-content ranged from 0.1 to ~28 at.% by changing the number of Ag pellets positioned on the pure Ti target.

It is also possible to notice that the increase of Ag content resulted in an overall enlarge of the films' thickness due to the corresponding increase of the deposition rate. As reported by Zakrzewska [15], the higher deposition rate should be related with the fact that the sputtering rate of noble metals is commonly higher than that found in compound targets, such is the case of the oxide passive Ti targets. The coatings in study were obtained in reactive mode, thus this phenomenon must be contemplated. However, the increasing fraction of Ag pallets on the Ti target will gradually reduce the poisoning effect, inducing a gradual enhancement of the deposition rate of the coatings.

All the coatings were submitted to thermal treatment at 500 °C. As was expected, no significant changes in the thickness and chemical profile of the coatings were obtained, since the annealing process was done in vacuum. On the other hand, the energy transferred during the

Table 1 Main characteristics of the as-deposited Ag:TiO_2 coatings

Sample	Ag content (at.%)	Thickness (μm)	Roughness (nm)
TiO_2	0	0.2	5.9
Ag #1	0.1	0.3	6.0
Ag #2	12.8	0.8	127.9
Ag #3	23.3	2.0	164.6
Ag #4	27.7	1.4	86.6

annealing processes will surely induce some structural and morphological changes into the films [13, 16, 17], as will be later described.

In respect to the as-deposited and as-annealed morphologies, the cross-section SEM micrographs of the coating are presented in Fig. 1. As a consequence of the thermal treatment, two main morphological modifications can be noticed. The first is directly related with the Ag content dispersed in the TiO_2 host matrix, while the second could be correlated with the structural and morphological rearrangements occurring as a result of the annealing process.

Upon the addition of Ag, the distinctive columnar structure of pure TiO_2 and Ag #1 was changed into a more disordered microstructure, less compact and relatively more porous (Fig. 1). The increasing Ag incorporation from Ag #2 to Ag #3, corresponding to ~13 and ~24 at.% Ag, respectively, leads to the formation of Ag clusters/aggregates, uniformly distributed on the coating's surface. Figure 1 evidences the presence of small Ag clusters surrounding larger ones, Fig. 1c_1), which might be an indication of Ag diffusion and its coalescence at the surface. These results are in accordance to those previously reported by other authors [13, 18–20]. The further increase of the Ag content leads to a significant change in the Ag #4 thin film morphology, presenting an atomic concentration of 27.7 at.% Ag, as can be seen in Fig. 1d_1). For this coating the columnar microstructure evolves to a more granular and compact one and is also well denoted the Ag clusters homogeneously distributed within the TiO_2 matrix. Moreover, the large Ag oblate agglomerates, observed in the films with low and intermediate Ag contents (samples Ag #2 and Ag #3 with 12.8 and 23.3 at.% Ag, respectively) seem to give rise to significantly smaller metallic spherical clusters on the coating's surface. This unusual morphology might be easily explained considering that ~28 at.% of the film composition is Ag, with only ~24 at.% of Ti. This means that during the coatings formation a significant amount of Ag metallic reaches the growing film (even exceeding Ti), creating favorable conditions for clustering. The research work of Torrel et al. [14] supports this idea by sustaining that small NPs clusters tend to be almost spherical whereas larger NPs had oblate form [10].

AFM images in Fig. 2 illustrate the surface morphology of Ag:TiO_2 thin films, supporting the observed morphological SEM evolution in the as-deposited coatings. The topography of the TiO_2 reference coating, Fig. 2a), follows the results obtained by Amin et al. [21]. The statistical mean roughness of 4.65 nm and the real area of 101.1 μm^2 sustenance the regularity of small size presented by the particles along the surface of the coating.

For coatings containing Ag addition, the AFM maps show that the surface roughness is directly dependent on the shape and size of the Ag clusters, which in turn is directly related with Ag content. For Ag #2 and Ag #3 samples, Fig. 2b, c) the larger Ag agglomerates at the surface increases the surfaces roughness (Table 1). Nonetheless, for the sample with the highest Ag content, Ag #4, this evolution trend changed. As can be seen in Fig. 2d) the surface roughness is much lesser than for other coatings. These results are in agreement with those present previously concerning morphological analysis.

Concerning the thermal effect on surface morphology, it is clear that outward diffusion was enhanced, leading to a clear gradient in Ag composition throughout the film thickness and to an increased size in Ag nanoclusters. The coatings microstructures are now heterogeneous, as can be seen in Fig. 1c_2, d_2). These results in addition to Ag content enlarge in the outermost regions of the coatings have been observed in other works [13, 14, 19]. The thermal treatment of the highest Ag content sample (Ag #4) leads to TiO_2 matrix crystallization. This structural variation enhances Ag diffusion along TiO_2 grain boundaries, although it was still possible to perceive Ag incorporation throughout the matrix (Fig. 1d_2).

Heat treatments are known to promote both diffusion and coalescence of Ag, but also the crystallization of the host matrix [13, 14, 17, 19]. Changes of shape, size, crystallinity and distribution of Ag agglomerates were endorsed to TiO_2 crystallization, as was observed by SEM analysis. The crystallization process of the matrix was particularly evident in the morphology of the TiO_2_TT and Ag #1_TT samples, Fig. 1a_2, b_2), evolving from porous and columnar microstructures to compact and granular ones.

In order to investigate how the correlation between the morphological and the topographical evolution influenced the overall films response, a detailed structural evolution on post-deposited, Fig. 3, and post-annealed samples, Fig. 4, was carried out by XRD analysis. The indexed crystal phases suggest that the thermal annealing process, by inducing the diffusion and the coalescence phenomena, leads to a progressive growth of the Ag clusters. This result is well established by the increasing definition of the Face-Centered Cubic, FCC, Ag-indexed diffraction patterns, especially notorious in the samples with higher Ag contents. The grain size evolution of the Ag nanoparticles can be easily being determined from Fig. 4. A clear decrease of the full width at half maximum (FWHM) of the narrower and more intense diffraction peaks is noteworthy, meaning well-defined FCC Ag structures and larger grain sizes of the metallic phase. Besides and alongside the preferential Ag orientation growth (111), new XRD diffraction peaks arise at $2\theta \approx 44.33°$ and $\approx 44.33°$ [ICDD card N° 004-0783] corresponding respectively to (200) and (220) FCC plans. This is particular noticed for the samples with higher Ag addition (Fig. 4).

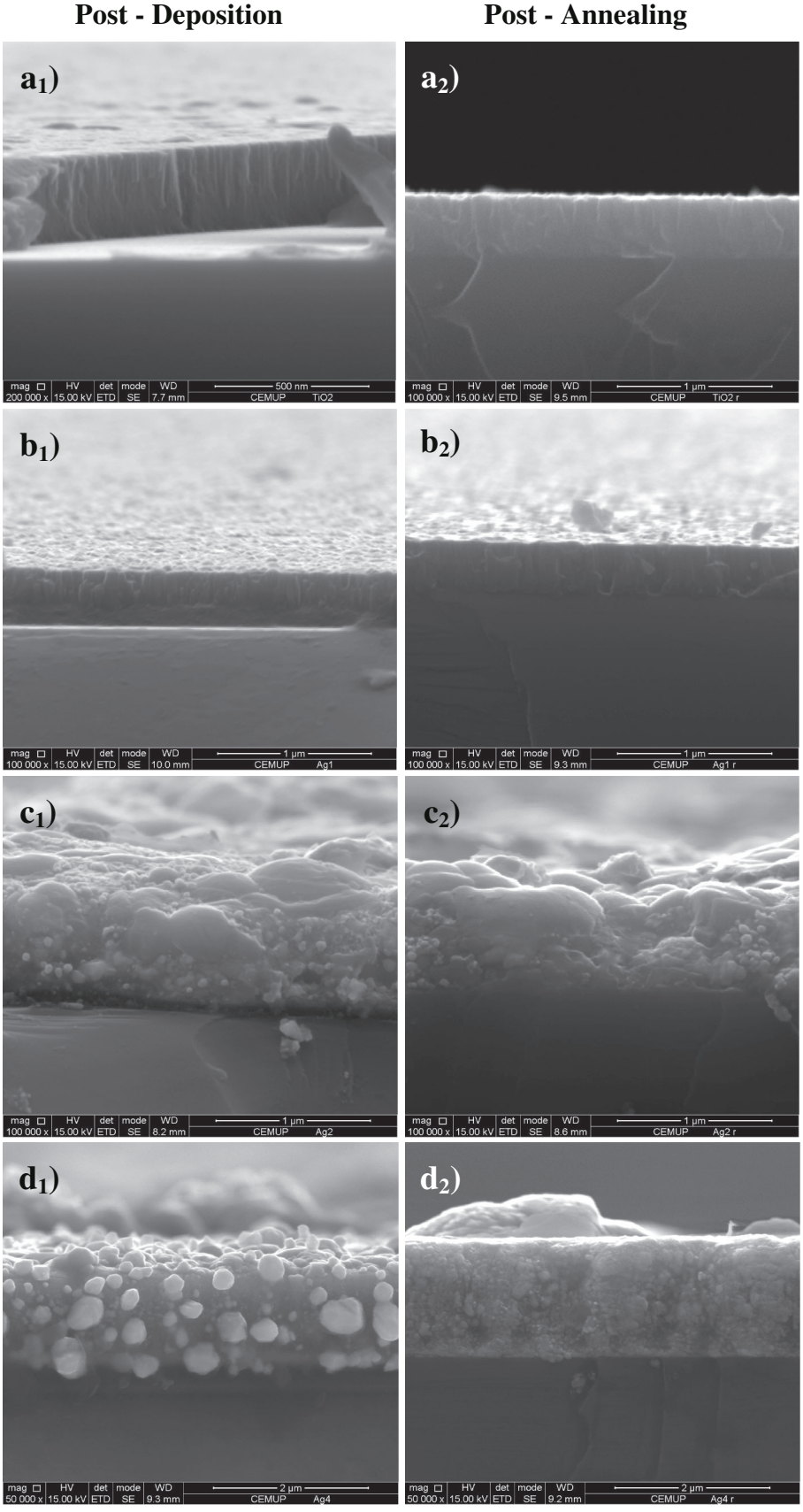

Fig. 1 SEM cross-section micrographs of the post-deposited (*left*) and post-annealed (*right*) samples with Ag contents of: **a** 0 at.% (TiO_2 reference); **b** ∼0.1 at.% (Ag #1); **c** ∼23.3 at.% (Ag #3) and **d** ∼27.7 at.% (Ag #4)

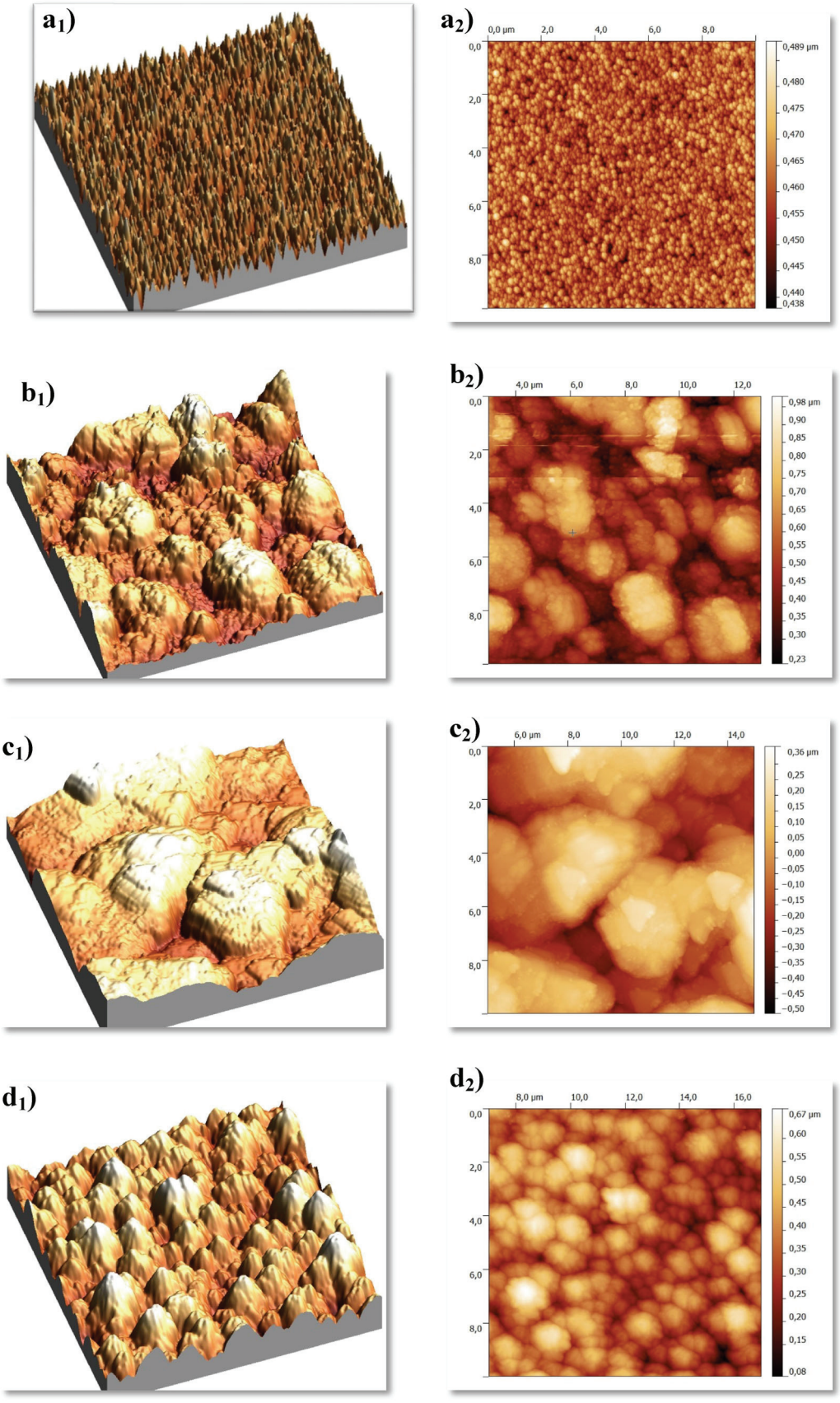
a1)
a2)
0,0 µm 2,0 4,0 6,0 8,0
0,0 2,0 4,0 6,0 8,0
0,489 µm 0,480 0,475 0,470 0,465 0,460 0,455 0,450 0,445 0,440 0,438
b1)
b2)
4,0 µm 6,0 8,0 10,0 12,0
0,0 2,0 4,0 6,0 8,0
0,98 µm 0,90 0,85 0,80 0,75 0,70 0,65 0,60 0,55 0,50 0,45 0,40 0,35 0,30 0,23
c1)
c2)
6,0 µm 8,0 10,0 12,0 14,0
0,0 2,0 4,0 6,0 8,0
0,36 µm 0,25 0,20 0,15 0,10 0,05 0,00 −0,05 −0,10 −0,15 −0,20 −0,25 −0,30 −0,35 −0,40 −0,45 −0,50
d1)
d2)
8,0 µm 10,0 12,0 14,0 16,0
0,0 2,0 4,0 6,0 8,0
0,67 µm 0,60 0,55 0,50 0,45 0,40 0,35 0,30 0,25 0,20 0,15 0,08

◀**Fig. 2** AFM images of as-deposited samples in 3D (*left*) and 2D (*right*) modes: **a** TiO_2 reference; **b** Ag #2; **c** Ag #3 and **d** Ag #4

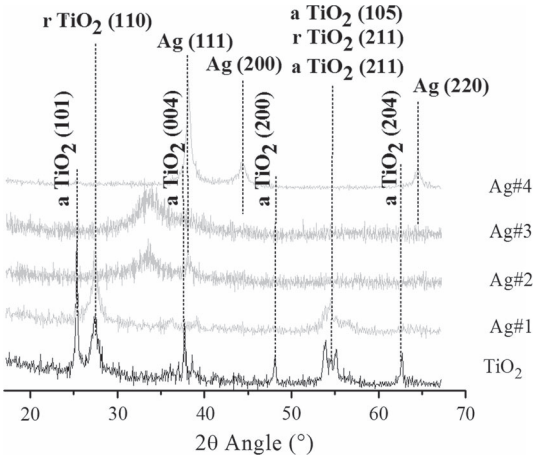

Fig. 3 Structural evolution of the as-deposited Ag:TiO_2 coatings, function of the increasing Ag content

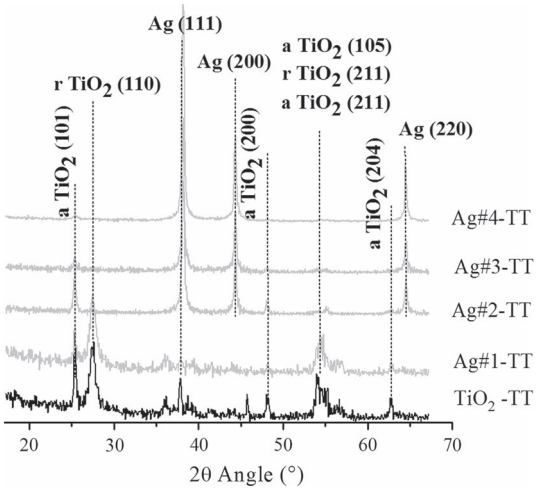

Fig. 4 Structural evolution of the annealed Ag:TiO_2 coatings, function of the increasing Ag content

Evidences of the FCC-type Ag crystalline structure can also be found in the as-deposited samples by the presence of (111) orientation Bragg peak, localized at $2\theta \approx 38.26°$. On a par also Ag #2 and Ag #3 coatings show similar features, but in these samples silver is probably dispersed in the amorphous TiO_2 matrix, due the broad and low intensity FCC diffraction peaks. These structural results are in accordance to those obtained by Okumu et al. [22], who suggest that the Ag dispersion by sputtering is an consequence of the impinging energetic oxygen ions formed during the Ag:TiO_2 grown.

Additionally, the XRD patterns confirm the already mentioned changes on the microstructure of the samples induced by the thermal annealing, namely a clear crystallization of the oxide dielectric matrix, as demonstrated by the diffraction patterns of anatase located at 25.29° and 48.19° [ICDD card N° 021-1272]. In the case of pure annealed TiO_2_TT and Ag #1_TT samples, Fig. 4, both tetragonal phases: anatase and rutile [ICDD card N° 078-1508], located at $2\theta \approx 27.63°$, could be detected. For higher Ag contents (≥13 at.%), the crystallization of TiO_2 at 500 °C in vacuum seemed to be delayed. It seems that the fine dispersion of silver in the amorphous TiO_2 matrix may inhibit the growth of the average particle size, being the extent of this inhibition dependent on the amount of Ag present in the matrix. The presence of Ag atoms seemed to increase the activation barrier for crystallization [13, 19], since during the sputtering process Ag became a physical barrier to confine the TiO_2 nanoparticles, i.e., TiO_2 nanoparticles would be surrounded and separated by the Ag atoms. Afterwards, the energy necessary for the movement of the grain boundary for merging TiO_2 nanoparticles increased and this phenomenon consequently inhibited the TiO_2 grain growth. In summary, the extent of such inhibition is dependent on how well the TiO_2 crystallites are separated, which correlates to the amount of Ag present in the films [23, 24].

3.2 Biological characterization

Silver is added to titanium dioxide thin films with two main purposes: to reduce the brittle-like character of TiO_2 films and to confer antimicrobial properties. These two features support the use of the developed Ag:TiO_2 thin films for applications such as top/protective coating to be used in pressure sensors for lower limb prosthesis, the main focus of the present work.

To study the ability to inhibit microbial growth of distinct TiO_2 thin films doped with different atomic percentages of Ag, an experimental protocol was designed, where sterile culture medium was incubated for 5 days at 37 °C with the sputtered as-deposited and thermal treated samples. Then, these conditioned media were inoculated and the microbial growth was monitored by optical density to obtain a growth curve. Death controls using kanamycin for both Gram positive and Gram negative bacteria, and fluconazole for *C. albicans,* were prepared in parallel. The relative specific growth rates presented in Fig. 5 were calculated as percentage of the specific growth rate, obtained from the negative control (microorganism grown in media previously incubated with glass), since preliminary assays confirmed that glass-conditioned medium did not inhibit the growth of the tested microorganisms. Two consecutive washing cycles were performed, with each piece of material, in order to have an idea of how stable their antimicrobial activity was.

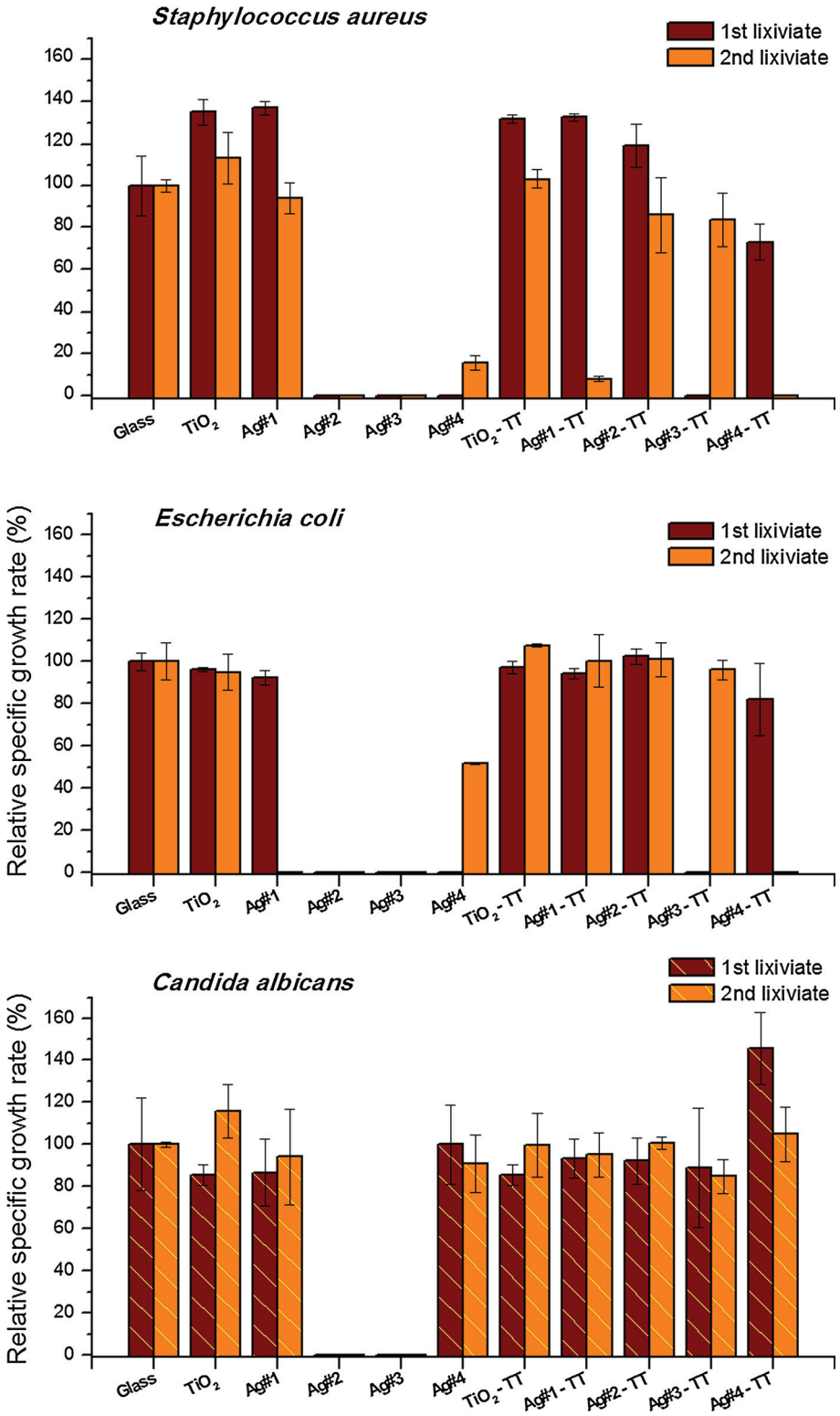

Fig. 5 Antimicrobial effect of Ag:TiO_2 thin films onto glass substrates, after deposition and after thermal treated, evaluated as the relative decrease in specific growth rate of each microorganism by indirect contact with a first and a second thin film washing

According to the results (Fig. 5), none of the extracts of TiO_2 held any antimicrobial property against *S. aureus*, *E. coli* and *C. albicans*. On the contrary, it was found that media previously incubated with Ag #2 and Ag #3 as-deposited films, completely inhibited the growth of bacteria and yeast. These results sustain that the antimicrobial effect is not significantly lost after two washing cycles of 5 days each, as tested. The media previously in contact with Ag #1 as-deposited film, obtained from both washing cycles were unable to inhibit the bacteria or the yeast, except for the 2nd extract that inhibit the growth of *E. coli*.

The same image (Fig. 5) reveals that Ag:TiO_2 thin films thermal annealed at 500 °C produced quite different results. *C. albicans* was not inhibited by none of the extracts. Only the first extract conditioned with Ag #3_TT inhibit the growth of both *S. aureus* and *E. coli*, but this property was lost in the second washing cycle. Ag #2_TT was no longer able to inhibit bacteria. The second extract from Ag #1_TT inhibits the growth of *S. aureus*. The Ag #4 films behaved surprisingly different from what it would be expected according to its highest content of Ag. In general, the liquid extracts obtained from this film were less efficient in preventing microbial growth when compared to Ag #3 or Ag #2 samples. The yeast growth was not affected by none of the tested Ag #4 liquid extracts. Regarding bacteria, Ag #4 and Ag #4_TT affected growth differently. For this particular thin film, the heat treatment seems to delay the diffusion of Ag to the liquid extract, since only the second liquid extraction significantly affected both Gram positive and Gram negative bacteria. Both the first and second lixiviates obtained from Ag #4 as-deposited coating have the capacity to decrease the relative specific growth rate but in the second "washing cycle" this capacity is diminished.

The results obtained suggested that the diffusion of Ag ions (Ag^+) or Ag^0 particles from the surface of the coatings to aqueous solutions is as a function of the silver content. As already mentioned, the annealing process did not affect the chemical composition in terms of amount of Ag present, but it affected the structure and the morphology of the Ag: TiO_2 system, promoted by rearrangements of Ag nanoclusters and by the crystallinity degree of the TiO_2 host matrix. These induced changes conferred some thermodynamic stability to the sintered system and diminished the diffusion of Ag outward the surface films when exposed to an aqueous environment. In general, it was found that above 12 at.% Ag, the films exhibit antimicrobial properties under the tested conditions, although this property was lost after heat treatment. Due to differences in the preparation and biological characterization methods, a direct comparison between these results and others is not straightforward. Yu et al. [25] have produced Ag:TiO_2 thin films with atomic percentages below 2.28, annealed at 500° C, all of which were described as having an antimicrobial effect against *E. coli*. Apart from the different method used to obtain the Ag:TiO_2 films, the bacteria suspension was in direct contact with the film which boosted the observed effect. Hsieh et al. [26], produced Ag:TiO_2 thin films by reactive sputtering in Ar + O_2 atmosphere, annealed at 500 °C. After 24 h, the films containing 7 and 10 at.% of Ag exhibit considerable antimicrobial activities.

A direct method, adapting the disc diffusion method, was also employed for the qualitative assessment of antimicrobial effect, of each material, including the glass control. The square pieces (2.25 cm^2) were laid on top of an inoculated 0.5 % agar overlay and a small growth inhibition halo was observed for *E. coli* and *S. aureus* around the two materials with the highest Ag content (data not shown). These results confirmed that only Ag #2, Ag #3 and Ag #4 as-deposited films exhibited, in fact, an antimicrobial effect.

Elemental silver and silver salts have been used for centuries as antimicrobial agents in health care [27]. Three main mechanisms of Ag and Ag salts antibacterial activity are currently proposed: uptake of free Ag ions followed by disruption of ATP production and DNA replication; generation of reactive oxygen species (ROS); and direct damage to cell membranes [11]. Ionic Ag has known antibacterial properties, thus, it is expected that ions eluted from silver nanoparticles are responsible for at least a part of their antibacterial properties. The diffusion of Ag ions will depend not only on the concentration but also on the structural and physical properties of Ag-containing material like particle size, shape, crystallinity, surface chemistry, and on the environmental conditions like pH, ionic strength and the presence of ligands [11]. Our results show that the antimicrobial behaviour of the Ag:TiO_2 films was determined both by Ag concentration and by heat treatment. As previously mentioned, upon post-annealing treatments, the samples went through meaningful variations in their structure and morphology (see Sect. 3.1). With the crystallinity improvement in both Ag nanoclusters and dielectric TiO_2 matrix, the system earns stability as a whole and the release of Ag to the aqueous environment was reduced. The methodology used to test antimicrobial activity (indirect approach using conditioned media) requires that the release of Ag, regardless of its oxidation state, must occur to achieve toxicity against the tested microorganisms.

Antimicrobial activity is common with heavy metals like lead or mercury, but Ag presents the advantage of being by far less toxic to humans. Even so, although metallic Ag being considered of minimal health risk, once at a nanoscale, some materials start to exhibit significant toxicity to mammalian cells [27].

To gain a general insight into the cytotoxicity of Ag:TiO_2 films, mouse primary embryonic fibroblasts (MEFs) were used as a mammalian cell model. The results obtained by testing the conditioned animal cell culture media mirrored the results of antimicrobial activity (Fig. 6). Extracts from one and five days-incubation of TiO_2 and Ag #1 thin films were not toxic to MEFs, compared to the glass control, even after 72 h of cell exposure. Extracts from Ag #2, Ag #3 and Ag #4 thin films induced more than 55 % reduction in MEFs viability after the first 24 h of exposure. Ag #4 led to complete death of MEFs. The fact that there was no significant difference between the extracts obtained after 24 h and 5 days may indicate

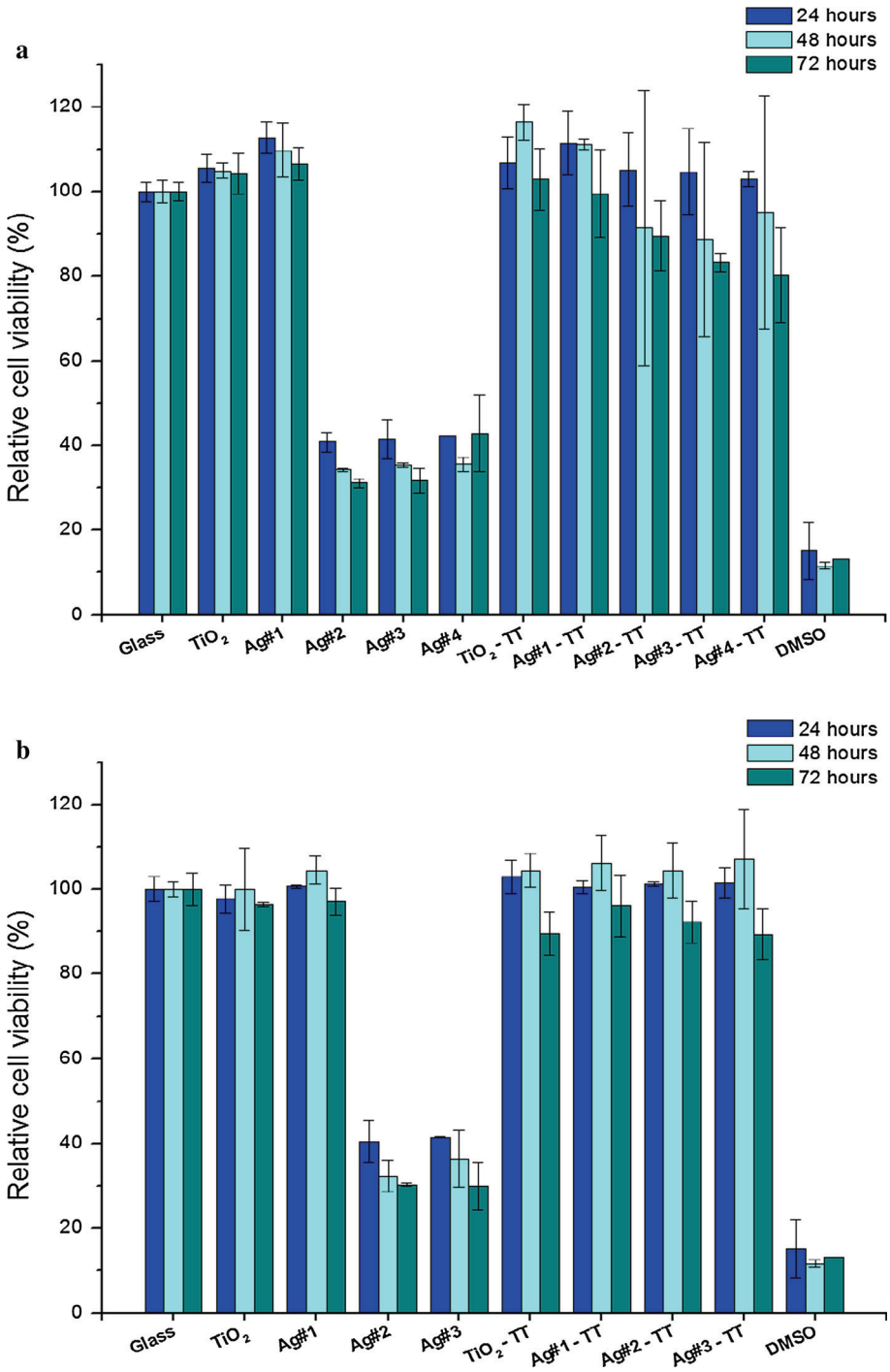

Fig. 6 Viability of mouse embryonic fibroblasts, MEFs, in previously conditioned cell culture media. The conditioning was performed at 37 °C by incubating sterile culture media one (**a**) and 5 days (**b**) with sterilised Ag:TiO_2 thin films, deposited onto glass substrates for as-deposited and annealed samples. The viability is obtained by comparison with the negative control (glass)

that the silver leaching attained the equilibrium in the first 24 h of medium conditioning. The conditioned media obtained by contact with annealed films were not toxic to MEFs when exposed for 48 h. After 72 h of exposure to media, previously conditioned for a day, the viability started to decrease but with no statistical significance.

By inductively coupled plasma mass spectrometry (ICP-MS), the presence of Ag in cell culture medium was confirmed in extracts conditioned with films with the highest silver contents—Ag #2, Ag #3 and Ag #4 (Table 2), after 24 h of contact at 37 °C. For TiO_2 and Ag #1 samples, it was not possible to detect any Ag in extracts by ICP-MS. The improvement in the crystallinity of the TiO_2 as well as the stability of Ag clusters inside the host matrix reduced Ag leaching from the film to the surrounding aqueous media, as given by the lower Ag

Table 2 Silver concentration in cell culture medium after 24 h in contact with Ag:TiO_2 thin films deposited onto glass substrates, as determined by ICP-MS

Sample	Ag content (mg/L)	
	As-deposited	As-annealed
Glass	0	0
TiO_2	0	0
Ag #1	0	0
Ag #2	1.31	0.26
Ag #3	1.84	0.45
Ag #4	1.23	0.86

concentrations found in extracts from these materials. As expected, for the post-annealing samples, the Ag release increased with Ag atomic percentage, but for the as-deposited thin films, the Ag release from Ag #4 was even lower than the amount released from Ag #2, which is in agreement with the film morphology, namely with size, shape and homogeneously distribution of Ag clusters along the TiO_2 matrix (see Sect. 3.1).

Since for biomedical applications, an intimate contact between the developed thin films and human skin is required, a complementary assay was performed to evaluate the potential induction of toxicity when in direct contact with normal human skin fibroblasts (BJ5ta cell line). The results indicate that Ag #2, Ag #3 and Ag #4 thin films were toxic to BJ-5ta cells (80 % reduction in cell viability at 24, 48 and 72 h of contact) (Fig. 7). In contrast to the previous test, Ag #1 film induced some toxicity after 48 and 72 h of contact. Another very interesting result regards the fact that, when in direct contact with fibroblasts, the annealed films induced the same level of toxicity as the as-deposited coatings. The higher toxicity can be attributed to the direct contact between cells and the material where intrinsic physical properties of the surface affects either the viability or the capacity of cells to adhere to the film. Since the surface physical properties of Ag #1 are not so different from the neat TiO_2 thin film. The results demonstrate that these cells in direct contact with the coatings can be affected by the presence of smaller amounts of Ag. When a toxic effect is observed, neither MEFs or BJ-5ta fibroblasts are able to recover over the 72 h of direct or indirect contact with the Ag:TiO_2 thin films.

Abundant research has been devoted to study the applicability of Ag antimicrobial properties, however most studies haveńt assessed the impact and toxicity of silver to relevant mammalian cell lines. The huge heterogeneity in sensitivity of different cell lines to a particular material is well known [12, 28], but frequently only one cell line is tested and often this cell line is not normal or primary. In this study, the authors tested primary cells (MEFs) and a human skin normal fibroblast cell line, given the final application of the produced Ag:TiO_2 thin films. Two different methodologies were used to evaluate the influence of direct and indirect contact between two different mammalian cell types and films, in culture media previously incubated with films containing leachable. In the attempt to obtain the best tuning of Ag:TiO_2 coatings properties, before in vivo testing, it is important to minimize cytotoxicity to mammalian and human cells but simultaneously maximizing the antimicrobial effect in vitro.

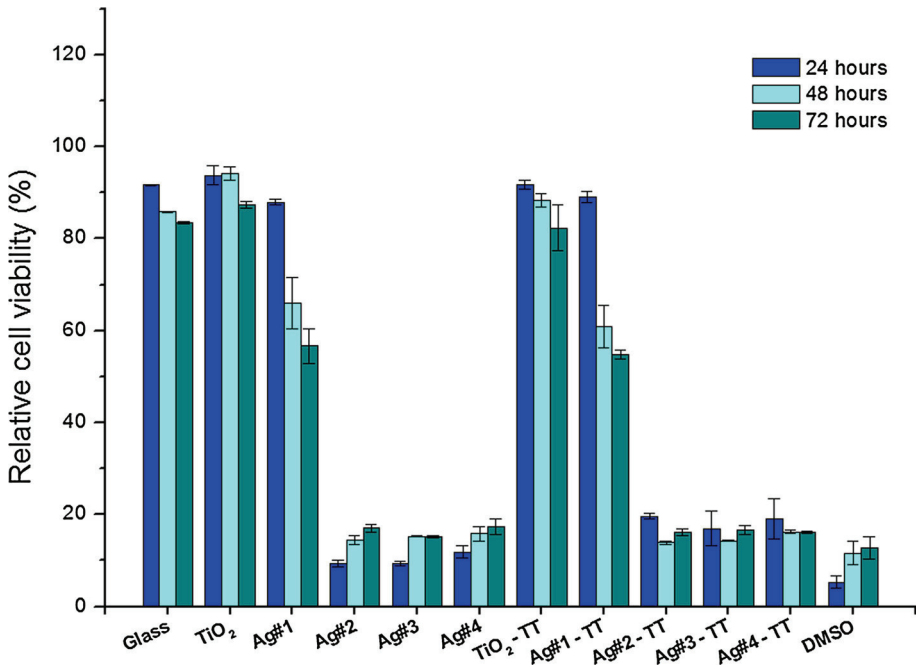

Fig. 7 Viability of hTERT-immortalized human foreskin fibroblast cell line, BJ-5ta, after contact with sterilised suspensions of CS, LS and CS-LS nanoparticles during 24, 48 and 72 h. The viability is obtained by comparison with the negative control (no treatment)

4 Conclusions

In this study the influence of Ag concentration on Ag:TiO_2 sputtered coatings properties was fully characterized. The assays were carried out in a dielectric titanium oxide matrix with Ag content ranging from 0.1 to ~30 at.%. The presence of Ag led to its diffusion and coalescence from the columnar boundaries of TiO_2 matrix towards the surface, noticeable by the denser coatings microstructure. Annealing treatments at 500 °C promoted Ag diffusion to a clear clustering process of the metallic NPs, increasing their agglomeration sizes. Additionally, the thermal treatment also produced changes on both Ag-NPs shape and matrix structure. The FCC structure of the noble metallic phase became more significant, but the anatase phase crystallization was delayed due to presence of Ag dispersion. The biological tests indicated that the as-deposited samples with Ag contents above 12 at.% displayed antimicrobial activity, which was partially lost after the heat treatment, as it reduced Ag release to the aqueous environment. Moreover, the results of antimicrobial activity were mirrored by the cytotoxicity for conditioned animal cell culture media.

Further studies should be carried out in order to characterize the stiffness and conductivity of Ag:TiO_2 thin films, since these features will determine their performance as a protective layer of sensors. This work highlighted the potential of silver nanoparticles to tailor TiO_2 matrix physical and biological properties and it was an essential step towards the assessment of the ideal Ag concentration for the protective layer interfacing between the human body and pressure biosensors, such as in prosthetic devices.

Acknowledgments This research is partially sponsored by FEDER funds through the program COMPETE—Programa Operacional Factores de Competitividade and by national funds through FCT—Fundação para a Ciência e a Tecnologia, under the projects PEst-C/EME/UI0285/2011, PTDC/SAU-ENB/116850/2010, PTDC/CTM-NAN/112574/2009P. T Matamá acknowledges FCT for Grant SFRH/BPD/47555/2008.

References

1. Song D-H, Uhm S-H, Lee S-B, Han J-G, Kim K-N. Antimicrobial silver-containing titanium oxide nanocomposite coatings by a reactive magnetron sputtering. Thin Solid Films. 2011;519:7079–85.
2. Sheel DW, Brook LA, Ditta IB, Evans P, Foster HA, Steele A, et al. Biocidal silver and silver/titania composite films grown by chemical vapour deposition. Int J Photoenergy. 2008;2008:1–11.
3. Foster HA, Sheel DW, Sheel P, Evans P, Varghese S, Rutschke N, et al. Antimicrobial activity of titania/silver and titania/copper films prepared by CVD. J Photochem Photobiol A. 2010;216:283–9.
4. Goharshadi EK, Azizi-Toupkanloo H. Silver colloid nanoparticles: ultrasound-assisted synthesis, electrical and rheological properties. Powder Technol. 2013;237:97–101.
5. Xu Y, Tang H, Liu JH, Wang H, Liu Y. Evaluation of the adjuvant effect of silver nanoparticles both in vitro and in vivo. Toxicol Lett. 2013;219:42–8.
6. Beer C, Foldbjerg R, Hayashi Y, Sutherland DS, Autrup H. Toxicity of silver nanoparticles: nanoparticle or silver ion? Toxicol Lett. 2012;208:286–92.
7. Grosse S, Evje L, Syversen T. Silver nanoparticle-induced cytotoxicity in rat brain endothelial cell culture. Toxicol in vitro. 2013;27:305–13.
8. Levard C, Hotze EM, Lowry GV, Brown GE Jr. Environmental transformations of silver nanoparticles: impact on stability and toxicity. Environ Sci Technol. 2012;46:6900–14.
9. Ahamed M, Alsalhi MS, Siddiqui MK. Silver nanoparticle applications and human health. Clin Chim Acta. 2010;411:1841–8.
10. Daniel SCGK, Tharmaraj V, Sironmani TA, Pitchumani K. Toxicity and immunological activity of silver nanoparticles. Appl Clay Sci. 2010;48:547–51.
11. Marambio-Jones C, Hoek EMV. A review of the antibacterial effects of silver nanomaterials and potential implications for human health and the environment. J Nanopart Res. 2010;12:1531–51.
12. Singh RP, Ramarao P. Cellular uptake, intracellular trafficking and cytotoxicity of silver nanoparticles. Toxicol Lett. 2012;213:249–59.
13. Adochite RC, Torrell M, Cunha L, Alves E, Barradas NP, Cavaleiro A, et al. Structural and optical properties of AgTiO_2 nanocomposite films prepared by magnetron sputtering. Optoelectron Adv Mater Rapid Commun. 2011;5:73–9.
14. Torrell M, Adochite RC, Cunha L, Barradas NP, Alves E, Beaufort MF, et al. Surface plasmon resonance effect on the optical properties of TiO_2 doped by noble metals nanoparticles. J Nano Res. 2012;18–19:177–85.
15. Zakrzewska K. Noble metal/titanium dioxide nanocermets for photoelectrochemical applications. Solid State Ionics. 2003;157:349–56.
16. Oh B-Y, Jeong M-C, Kim D-S, Lee W, Myoung J-M. Post-annealing of Al-doped ZnO films in hydrogen atmosphere. J Cryst Growth. 2005;281:475–80.
17. Torrell M, Machado P, Cunha L, Figueiredo NM, Oliveira JC, Louro C, et al. Development of new decorative coatings based on gold nanoparticles dispersed in an amorphous TiO_2 dielectric matrix. Surf Coat Technol. 2010;204:1569–75.
18. Arcos TDL, Oelhafen P, Aebi U, Hefti A, Düggelin M, Mathys D, et al. Preparation and characterization of TiN–Ag nanocomposite films. Vacuum. 2002;67:463–70.
19. Adochite RC, Munteanu D, Torrell M, Cunha L, Alves E, Barradas NP, et al. The influence of annealing treatments on the properties of Ag:TiO_2 nanocomposite films prepared by magnetron sputtering. Appl Surf Sci. 2012;258:4028–34.
20. Oh J-H, Lee H, Kim D, Seong T-Y. Effect of Ag nanoparticle size on the plasmonic photocatalytic properties of TiO_2 thin films. Surf Coat Technol. 2011;206:185–9.
21. Amin A, Köhl D, Wuttig M. The role of energetic ion bombardment during growth of TiO_2 thin films by reactive sputtering. J Phys D Appl Phys. 2010;43:405303.
22. Okumu J, Dahmen C, Sprafke AN, Luysberg M, von Plessen G, Wuttig M. Photochromic silver nanoparticles fabricated by sputter deposition. J Appl Phys. 2005;97:094305.
23. Yuan Y, Ding J, Xu J, Deng J, Guo J. TiO_2 nanoparticles Co-doped with silver and nitrogen for antibacterial application. J Nanosci Nanotechnol. 2010;10:1–7.
24. Zheng J, Yu H, Li X, Zhang S. Enhanced photocatalytic activity of TiO_2 nano-structured thin film with a silver hierarchical configuration. Appl Surf Sci. 2008;254:1630–5.
25. Yu B, Leung KM, Guo Q, Lau WM, Yang J. Synthesis of Ag–TiO_2 composite nano thin film for antimicrobial application. Nanotechnology. 2011;22:115603.

26. Hsieh JH, Yu RB, Chang YK, Li C. Structural analysis of TiO_2 and TiO_2–Ag thin films and their antibacterial behaviors. J Phys. 2012;339:012012.
27. Chen X, Schluesener HJ. Nanosilver: a nanoproduct in medical application. Toxicol Lett. 2008;176:1–12.
28. Park MV, Neigh AM, Vermeulen JP, de la Fonteyne LJ, Verharen HW, Briede JJ, et al. The effect of particle size on the cytotoxicity, inflammation, developmental toxicity and genotoxicity of silver nanoparticles. Biomaterials. 2011;32:9810–7.